23

Digitally Fast Programmable Optical Signal Processing Devices

Xinwan LI, Zehua HONG, Shuguang LI and Jianping CHEN
Shanghai Jiao Tong University
P.R.China

1. Introduction

Optical delay, buffering, filtering, and switching are very important devices in both of optical communications and optical sensing areas. In order to decrease the cost of optical signal transferring/switching for digital data or analogue sensing signal, easy way is to increase the bandwidth utilities of optical communication/sensing systems to support mountains of users, like computers, sensor nodes in one network. However, the dynamic abilities of the above devices are becoming a big challenge, and which are also the bottle-neck in available technologies. This chapter presents a comprehensive review and overview on the cutting-edge frontier science and engineering of fast digital optical signal processing application. It discusses on the theory, design, fabrications of several typical examples of digital optical signal processor (DOSP) devices, which is in the form of semiconductor optical amplifier (SOA) and optical fibre delay lines (OFDL). The issues include the fast programmable optical fibre true delays, the fast programmable optical fibre buffer, the digital optical wavelength selective switches, etc.

2. Programmable optical fibre true delay (Li, 2007)

In last several years, the programmable optical fibre true delay has shown its powerful application abilities in microwave photonics and other areas. One typical example is the application of optical fibre delay lines as a notch filter replacing the traditional radio frequency (RF) signal processing to carry out the unwanted signals from the targets in the moving target identification ground radar system. In this section, we will introduce a kind of feed-forward optical fibre delay lines.

2.1 Brief review of optical fibre delay lines (OFDLs)

Programmable optical fibre delay lines (OFDLs) have many applications, such as antenna beam forming in phase array radar system(Seeds, 2006) and microwave signal processing(Capmany, 2005; Wilner, 1976), due to various advantages in comparison with the traditional electronical methods. It can provide true delay of microwave signal, very high product of time-bandwidth, immunization to electromagnetic interference (EMI) and

the possibility of spatial and wavelength parallelism by using WDM techniques. So far, two types of optical fibre delay lines have been proposed as buffers for optical packet communication networks: re-circulating type and traveling-wave type(Chang, 2006). Re-circulating buffers are compact and require fewer components to implement. However, the fibre loop length is fixed and hence it is not suitable for applications in phase array radar system and microwave signal processing. Traveling-wave buffer has the potential for the above applications, which will be introduced in thefollowing section. It can be cascaded to provide desired delay using, e.g., 2×2 optical switches or broadcast-and-select configuration (Chang, 2006). Of course, high-speed (≤1ns) and low-loss (≤1dB) optical switches are required(Seeds, 2005; Seeds2002).

Two typical high speed devices, i.e. $LiNbO_3$ switch(Murphy, 1996) and semiconductor optical amplifier (SOA) ON–OFF gate, can be considered. For $LiNbO_3$ 2×2 switch, the large insertion loss, polarization dependence and crosstalk need to be addressed before they can be used in phase array radar system and microwave signal processing. SOA ON–OFF gate has nanosecond switching speed, large on-off extinction ratio and wide optical bandwidth. It seems more suitable for traveling-wave type of fibre delay lines(Yeo, 2004).

In this section, we proposed a novel 3^n feed-forward OFDL using SOAs as switching components. Theoretical analysis and experimental verification are presented. Important issues, such as the attenuation(Moslehi, 1992), polarization, delay precision, and etc., are addressed in detail(Capmany, 2006; Ho-Quoc, 1996).

2.2 Design of k^n feed-forward optical fibre true delay line

Traditionally, the programmable traveling-wave fibre delay line is implemented by using 1×N optical switch, or equally by using 1×N coupler plus on-off gate (e.g. SOA) in each arm, as shown in Fig. 1(a)(Blumenthal, 1994). In this configuration, the maximum number of possible delays, y, is equal to the mount of SOAs, x. It is apparently not suitable to be scaled for large delays. The delay performance can be enhanced by configuring it in an alternative way with 2×2 switches(or 2×2 couplers plus ON-OFF SOA gates) and same number of SOAs as shown in Fig. 1(b). In this configuration, the total number of delays can be expressed as follows:

$$y = 2^{x/2} \tag{1}$$

where the number of SOAs, x, is supposed to even. We define such structure as 2^n structure, where, $n=x/2$, is the number of stages.

Similarly, we can use x SOAs to build k^J structure as shown in Fig. 1(c), where k is the dimension of each stage and J is the number of stages($J=x/k$ is an integer). It can be derived the total number of delays, y, is given by:

$$y = k^{x/k} \tag{2}$$

Equation (2) can be rewritten as:

$$\frac{\log(y)}{x} = \frac{\log(k)}{k} \tag{3}$$

Equation (3) shows that for the same x, there is an optimal k that gives maximum y. We use $L(k)$ to express the right side of Equation(3):

$$L(k) = \frac{\log(k)}{k} \tag{4}$$

The peak value of $L(k)$ can be obtained mathematically by differential operation on $L(k)$ as follows:

$$\frac{dL(k)}{dk} = 0 \tag{5}$$

So, the k can be obtained by solving Equations (4) and (5):

$$k = e = 2.718 \tag{6}$$

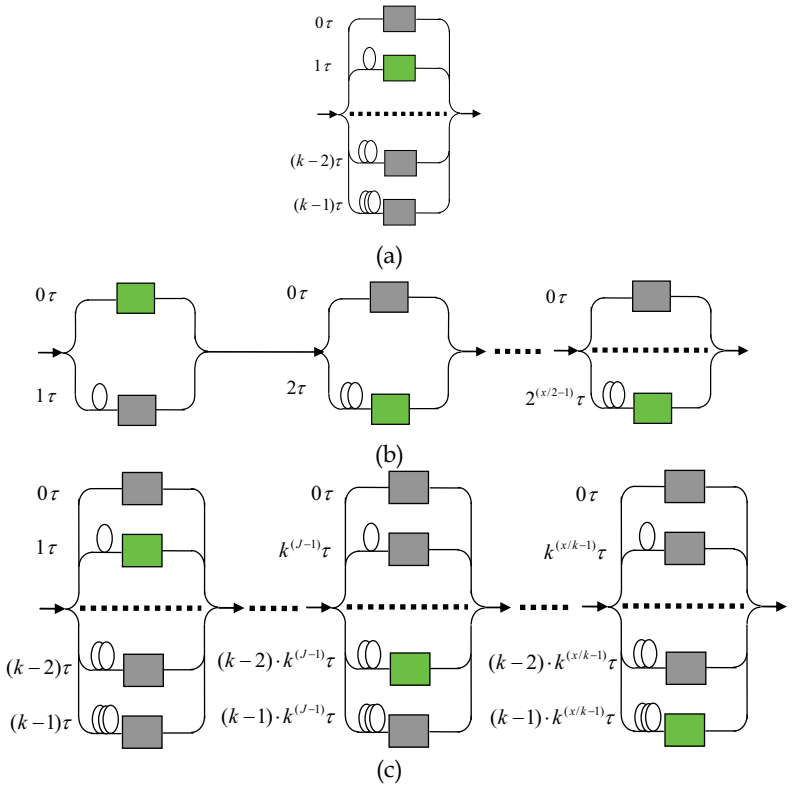

Fig. 1. The architectures of traveling-wave fibre delay lines
($y=x$ for (a), $y=2^{x/2}$ for (b), and $y=k^{x/k}$ for (c), where y is the maximum number of possible delays, and x is the number of SOAs)

However, as shown in Fig. 1, the physics meaning of k is the number of delay lines in each stage, so, k should be integer. Fig. 2 shows the relationship between $L(k)$ and k. It can be easily found that the optimal value k is 3. It can also be proved that 4^n structure is exactly the same as 2^n structure:

$$y(x) = k^{x/k} \xrightarrow{k=4} y(x) = 4^{x/4} = (2^2)^{x/4} = 2^{2\cdot x/4} = 2^{x/2} \rightarrow k = 2 \tag{7}$$

When the number of SOAs used is small, the difference between the maximum numbers of delays available for k=2 and k=3, respectively, are also small. However, as more SOAs are used, the difference becomes significant, as shown in Fig. 3. From the figure, we can see that fast tunable true delay line with large number of delays can be obtained by employing 3^n structure and certain number of SOAs. Fig. 4 shows the structure of 3^n delay lines, and Table 1 shows the delays of two stages from 0τ to 8τ respectively.

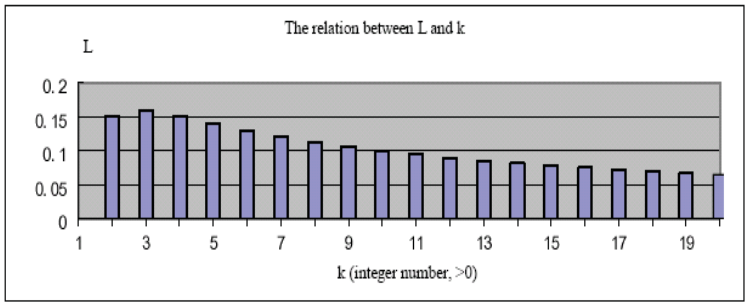

Fig. 2. $L(k)$ as a function of k

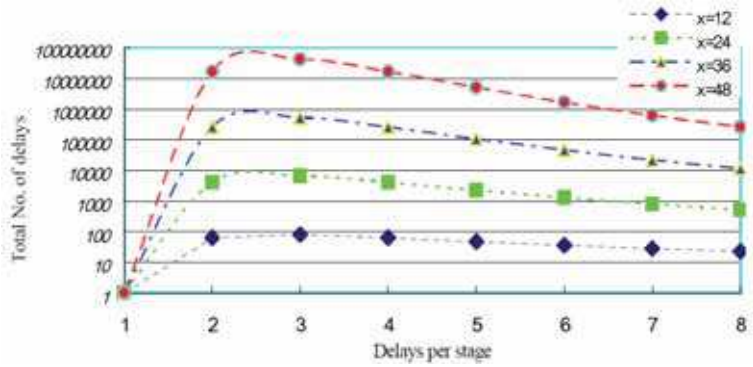

Fig. 3. Dependence of total delay number on the delay units per stage (x: the number of SOAs)

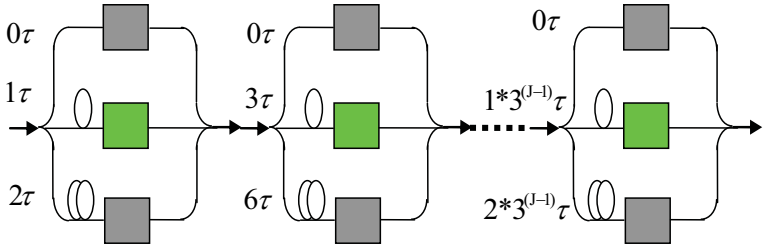

Fig. 4. The structure of 3^n delay lines

Total delay	Stage 1 (0τ, 1τ, 2τ)	Stage 2 (0τ, 3τ, 6τ)
0	0	0
1τ	1τ	0
2τ	2τ	0
3τ	0	3τ
4τ	1τ	3τ
5τ	2τ	3τ
6τ	0	6τ
7τ	1τ	6τ
8τ	2τ	6τ

Table 1. Delays of two stages from 0τ to 8τ in series

2.3 Implementation and performance measurement

According to the above analysis, 3^n feed-forward optical fibre true delay line based on SOAs can provide large amount of delays with fast tunability and easier scalability. For practical applications, problems such as insertion loss and polarization dependence should be considered. The former can be overcome by SOA itself for it provides gain in addition to ON-OFF gating. In fact, this is also one of advantages of employing SOAs. For the factors of the polarization dependence in optical fibre and in SOAs, we use Farady rotation mirrors (FRMs) to alleviate it. The SOAs we used are bi-directional SOA without inside optical isolators at input and output. Due to the low backward reflection of the SOA and the polarization rotation by FRM, no oscillation can be observed. Fig. 5 shows the structure for practical implementation and we built a two-stage (the first two stages in the experiment in hand) feed-forward optical fibre true delay line for experimental verification. For each stage, the light is fed from the input port of the optical circulator. It experiences delay whose amount is determined by turning on one of the SOAs and is then forwarded to the next stage via the output port.

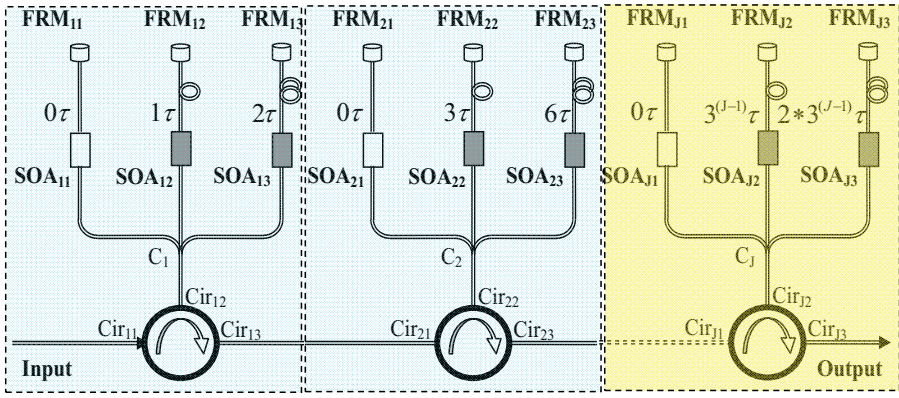

Fig. 5. A practical structure of 3^n feed-forward optical fibre true delay line

The main insertion loss is caused by 1×3 coupler. The light beam passes the coupler twice and experience about 12 dB loss (excluding the coupler's excess loss). By taking the losses resulted from the FRM and the circulator into consideration, the total loss of each stage is around 13 dB. It should be noted that the beam also passes SOA twice. Usually, an SOA can provide with 5-8 dB gain for small optical signals, e.g. -10dBm, under moderate drive current (~ 80mA). Therefore, by careful design of the drive current of each SOA, it is possible to obtain a delay stage with no insertion loss. This feature is particularly important for practical applications. It enables the proposed structure to be cascaded without limitation on the stage number.

The resolution is another key issue to be addressed. The delay introduced by a light path distance of 0.15mm, or fibre length of 0.103mm (group refractive index of 1.46 is supposed), is about 0.5 ps. It corresponds to a phase control precision of about 1.8° in X-band (λ ~ 3cm). In order to reach the above precision level, we used hydrogen flame to precisely adjust the fibre length, with the help of the high precision reflectometer (HP8504)(Shi, 2006). This equipment is used to precisely measure the lightpath difference between the measured arm and reference arm of Michelson interferometer. The measurement span (equivalent distance in air) is up to 400mm with resolution of 20 μm. Fig. 6 show the delay length measurements scheme using high precision reflectometer (HP8504).

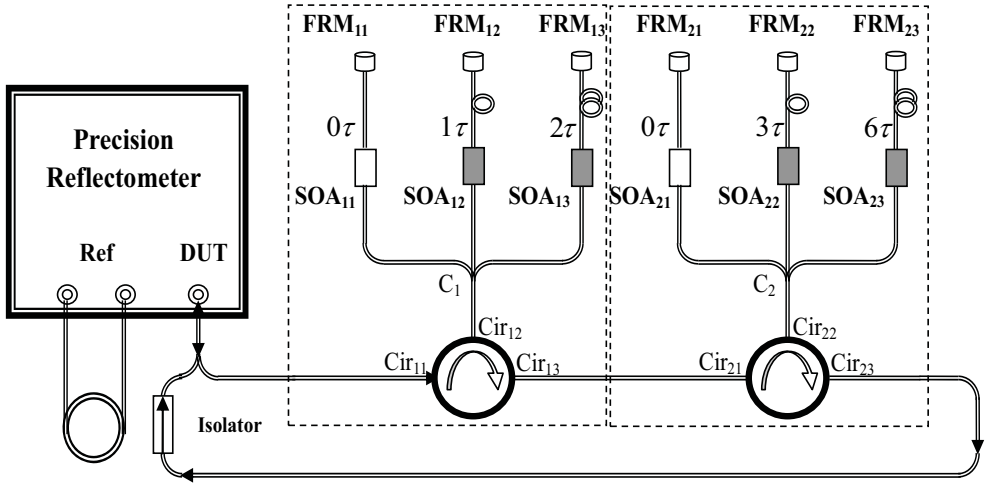

Fig. 6. The delay length measurements scheme

Fig. 7 shows the result when we set all six SOAs ON. It can be clearly seen that there are 9 peaks, which represent the all possible delays to be obtained, and each delay can be programmablely switched by setting of the relative one SOA per stage. The measured relative light path distances in three arms of the first stage are 20.756mm, 20.914mm, 21.056mm, respectively. The correspondent fibre lengths are 14.216 mm, 14.325mm, 14.422mm, respectively. These data indicate that τ as shown in Fig. 7 is 0.5 ps and the precision is kept within 0.03ps. One may note that there are insertion losses in stages 2 and

3. This is because of the limited drive current of the circuit we used, resulting in small SOA gain incapable to compensate the inherent insertion loss mentioned above.

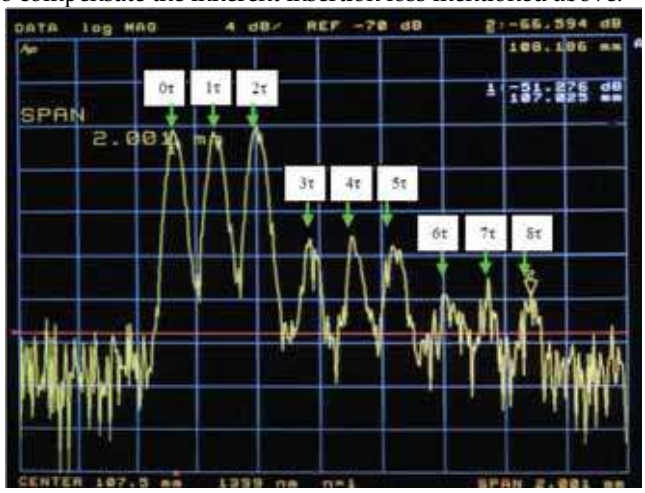

Fig. 7. Measured result of relative fibre lengths
x-axis: light path difference(0.2 mm/div), *y*-axis: relative intensity of the output(dB)

Fig. 8 and Fig. 9 show the measurement schemes and results of tuning speed respectively. The rise time is 18.6 ns and the fall time is 39.4 ns. Such speed can enhance the scanning performance of microwave significantly. The scanning frequency may be improved from tens of kHz up to 10 MHz. The drive circuit for the SOAs was implemented with conventional electronic devices at hand. There is large potential to improve the tuning speed, especially the switching-off performance. One may note that there is extra delay in switching-off process, which is mainly resulted in from the large junction capacitance in the device.

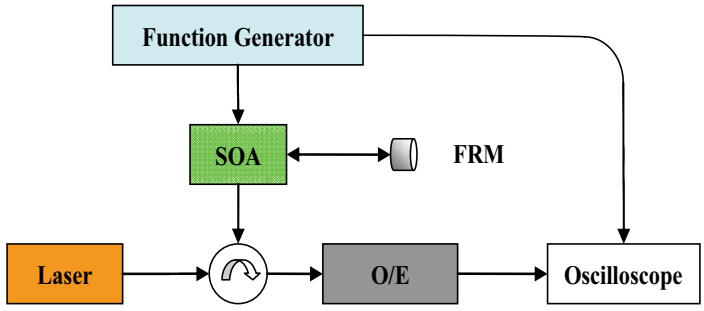

Fig. 8. The measurement scheme of tuning speed

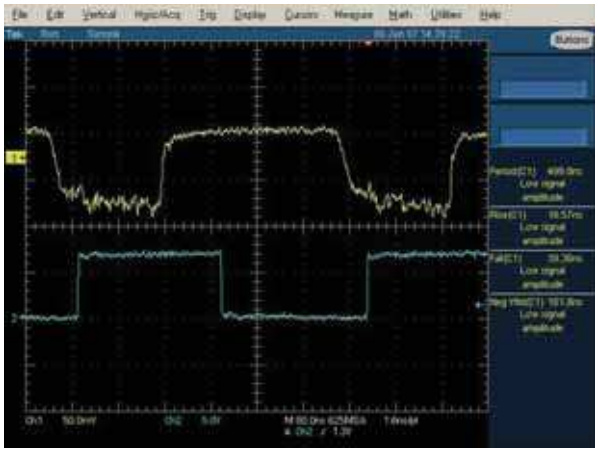

Fig. 9. Photograph of tuning speed measurement
(lower trace: drive pulse, upper trace: optical output)

We also measured the polarization dependence loss (PDL) using polarization controller. The measured result is 0.18 dB. In comparison with the PDL of SOA (~0.3dB), there is improvement that is mainly due to the employment of FRM. Fig. 10 shows the experiment scheme of measuring the polarization dependence loss (PDL).

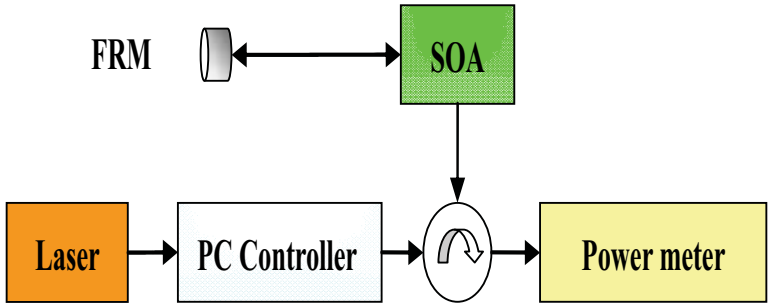

Fig. 10. The experiment scheme of measuring the polarization dependence loss

The relatively low noise figure of the SOA may bring a certain limitation to the proposed structure for some applications, especially for those requiring high transmission SNR. This indicates that for expansion purpose, noise performance should be taken into consideration, which is a topic worthy of intensive study and, however, beyond the scope of the paper. The following Table.2 exhibitis the description of five specifications. From the Table. 2, we can see that the insertion loss and polarization dependent loss are very low, and the switch speed of ON/OFF is are very fast, meanwhile we can use small number of SOAs to obtain large number of delays in series.

Specification		Description
Insertion loss		<1dB
Switch speed	Rise time	18.6ns
	Fall time	39.4ns
Polarization dependent loss		0.18dB
Delay efficiency		Small SOAs to obtain large delays
Delay precision		1ps, error <10%

Table 2. Specification of 3^n feed-forward optical fibre delay lines

3. Fast programmable travelling-wave buffer (Li, 2008)

The novel structure mentioned in the second section can be applied for a fast programmable traveling-wave buffer with a re-circulating one. The round trip time of the loop can be controlled as wanted.

3.1 Brief Introduction of traveling-wave buffer

As well known, the fast programmable optical buffering is quite an important technique to provide dynamic delay for photonic packets in an optical switching node. So far, two types of optical fibre delay lines have been proposed as buffers for optical communication networks: the re-circulating and traveling-wave structures (Chang, 2006) as addressed in the second sections of this chapter. Re-circulating buffers are compact and require fewer components to implement. However, the fibre loop length is fixed and hence the delay can only be the multiple of the round trip length of fibre loop. Traveling-wave buffers have the potential to avoid the above limitation. It can be cascaded to provide desired delay using, e.g., 2×2 optical switches or broadcast-and-select configuration(Blumenthal, 1994; Murphy,1996). However, large delay requires tremendous fibre length, which results in bulky structure. In this section, we present a novel structure, which combines a fast programmable traveling-wave buffer with a re-circulating one. The round trip time of the loop can be controlled as wanted. Such structure is applicable to optical packet switching, especial to optical burst switching, and also to other fields such as microwave photonics. In order to obtain high systematic performance, fast (e.g., ≤1ns) and low-loss (e.g., ≤1dB) optical switches are required(Blumenthal, 1994).

3.2 The principle and implementation

The proposed structure is shown in Fig.11. The optical fibre loop is interconnected via a 2×2 optical switch to the input and output. In order to support high speed switching, LiNbO3 switch(Murphy, 1996) can be used. In the loop, there are M in-fibre optical circulators, each of which connects a stage of delay lines via a 1×3 coupler. In each stage, the amount of delay is selected by one of the gated semiconductor optical amplifiers (SOAs) on three delay units (e.g. 0τ , 1τ and 2τ) with a Faraday rotation mirror (FRMs, marked as M in Fig.11) at each end. Each stage can be regarded as a programmable traveling-wave delay line. It has been found that the total number of delays for the J stages of delay lines can be expressed as Equation (2)(Li, 2007). The relation among x, y and k is shown in Fig.12. For the same

amount of total delays, the minimum number of SOAs needed can be found in the case of k=3. Hence, each stage containing three delay lines is the optimal structure.
With the proposed J-stage traveling-wave fibre delay line embedded in a re-circulating loop, the total number of delays per loop, N, can be expressed as:

$$N = 3^{x/3} \tag{8}$$

And the maximum delay per loop is

$$\tau_{total} = \tau_R + \tau \times 3^{x/3} \tag{9}$$

where, τ_R is the reference delay induced in the loop excluding the traveling-wave delay lines. The number of SOAs, x, is supposed to be the multiples of 3.

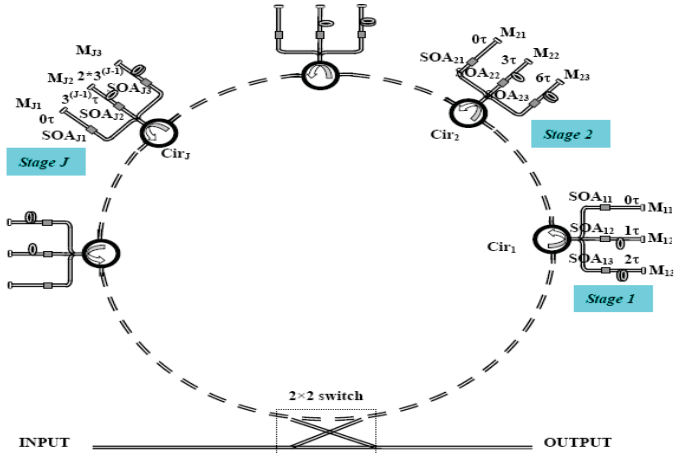

Fig. 11. The layout of re-circulating structure embedded with traveling-wave delay

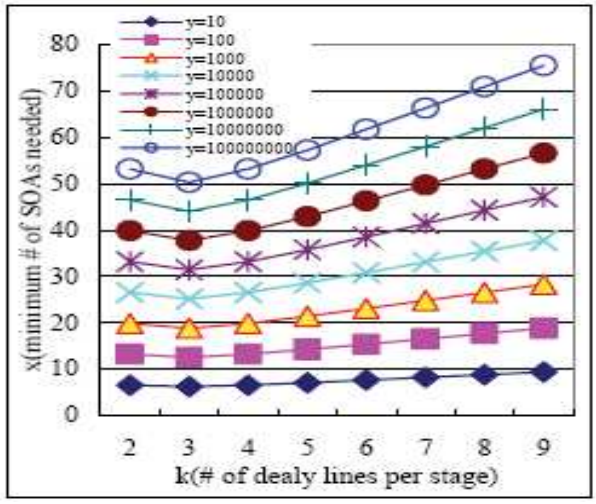

Fig. 12. The relation among the x, y ,and k

Next, we will analyze some properties of this buffer structure, such as the insertion loss, polarization dependent loss, the resolution of the fibre delay lines, and the tuning speed.
SOAs are used here to compensate the insertion loss mainly induced by couplers(excluding the coupler's excess loss). Because of the potential gain of SOA, it is possible to obtain a delay stage with no insertion loss. We use FRM here decrease the polarization dependent loss(PDL) for the polarization's elimination of FRM.
Several experiments have been carried out. The first is the length measurement with high precision reflectometer (HP8504)(Shi, 2006)of different buffer route. This scheme includes two stages of the buffer unit with six arms, and the results are the same as the second section, for we used the same basic fibre delay lines structure. The measured relative light path distances in three arms of the first stage are 20.756mm, 20.914mm, 21.056mm, respectively. The correspondent fibre lengths are 14.216 mm, 14.325mm, 14.422mm, respectively. These data indicate that τ as marked in Fig. 7(same delay lines used for these two applications: feed-forward OFDLs in section 2 and programmable optical buffer in this section) is 0.5 ps and the precision is kept within 0.03ps.The loop length was measured as 532 ps excluding the traveling-wave delay induced in each stage, which can be multiplied by re-circulating. The second experiment is about the tuning speed. The rise time is 17.7 ns and the fall time is 31.3 ns. The drive circuit for the SOAs was implemented with conventional electronic devices at hand. There is large potential to improve the tuning speed. Also the gain of SOAs was not optimized due to the limited drive ability of the circuit (one may note there are relatively large insertion loss, which can be overcome via the careful increase of the drive current). For this structure, we also measured the polarization dependence loss (PDL) using polarization controller with the result of 0.18 dB. Compared with the PDL of SOA (~0.3dB), there is improvement due to the employment of FRM.

4. Digitally tunable optical filter based on DWDM thin film filters and semiconductor optical amplifiers (Li, 2005)

Tunable optical filters have important application in fibre optic communications and other optical fields. Tuning ability is usually achieved by introducing extra phase shift via the electro optic, thermo optic, acoustic optic or piezoelectric effect, etc. The most commonly component for phase shift is interferometric structure(Sadot,1998) such as Fabry-Perot (FP), Mach-Zehnder (MZ) and Michelson interferometer. Those device based on interferometric structure have the similar defect — instability in operating wavelength, so the electronics should be adapted to stabilize the central wavelength.
Other kinds of tunable optical filters, digitally tunable optical filters (DTOFs)(Ishida, 1997), which can get over the problem of instability, have received widely attentions. One of DTOF structure based on arrayed waveguide grating (AWG) has been reported (Glance,1996; Zirngibl, 1994; Glance, 1994). Compared with the interferometric structure consisting of FP, MZ or Michelson interferometer, the AWG offers the advantages of low losses, high port counts, and mass productivity. However, AWG usually suffers the problem of temperature dependence, so the DTOF based on AWG may require precision thermal control. Another DTOF based on DWDM thin film filters (TTFs) and semiconductor optical amplifier (SOA) show the very stable characteristic in temperature performance. Furthermore it requires less SOAs to achieve the same wavelength tuning range in comparison with the reported structure(Zirngibl, 1994; Glance, 1994). Next, this structure will be introduced in detail.

4.1 The configuration of this digitally tunable filter

Fig. 13 shows the experimental configuration of the proposed DTOF. It consists of eight DWDM TTFs, six SOAs, one 1×2 splitter and one 4×1 combiner. Each of the TTFs is used as 1×2 or 2×2 wavelength selection element, as depicted in Fig. 14, depending on the position in the structure. For the 1×2 structure, we used a dual fibre collimator as one pair of input/output fibre ports and a single fibre collimator as the second output port. All the wavelengths from the input fibre will be reflected to the dual fibre collimator output, except for the wavelength which is equal to the center wavelength, λ_i, of the TTF (thin film filter). This wavelength will pass through the filter and arrive at the second output. In the 2×2 structure, we used another single fibre collimator as the second input. The work principle of the 2×2 structure is the same as the 1×2 one. Because the TTF only allows one wavelength to pass through, the wavelengths of the two input ports are arbitrary, i.e., independent of each other. In the DTOF of the proposed, TTFs of λ_2, λ_4, λ_6, λ_8 are set as 2×2 wavelength selection element, TTFs (thin film filters) of λ_3, λ_5, are set as 1×2 wavelength selection element, and TTFs of λ_1, λ_7 function as optical filters. The eight TTFs are connected in the order as shown in Fig. 13.

The input light to the DTOF is divided into two portions via the splitter and is firstly "selected" by SOA_{11} or SOA_{12}. For example, when SOA_{11} is turned on (SOA_{12} is off), all the wavelengths will arrive at the thin film filter with center wavelength of λ_2 and only one wavelength, namely λ_2, will pass through the filter, all the other wavelengths will be reflected and arrive at the subsequent TTFs (thin film filters). SOA_{2i} (i=1, 2, 3, 4) performs the second "selection" of wavelengths. In the above case, λ_2 will arrive at the output through the 4×1 combiner if SOA_{21} is on. The control table is listed in Table 3. In the table, "1" means that the SOA is turned "ON" and "0" means that the SOA is turned "off". It can be seen that this structure allows the center wavelength to be arbitrarily selected among the eight TTF wavelengths. For example, the DTOF is set at λ_1 with SOA_{12} and SOA_{21} "ON". The routing path for λ_1 is as follows: Input (multiple wavelengths) → SOA_{12} (ON) → λ_4 (Reflection) → λ_5 (Reflection) → λ_8 (Reflection) → λ_1 (Transmission) → λ_2 (Reflection) → SOA_{21} (ON) → Output.

The above configuration can be expanded to larger size. The expansion will not bring additional insertion loss for every wavelength undergoes transmission or reflection at most five times (four reflections and one transmission), independent of the filter size (i.e., the number of wavelengths). Of course the TTFs should be rearranged, i.e. configured as 1×2 or 2×2 structures according to the scale.

The number of SOAs to be used, which is important for cost consideration, is determined as follows. Suppose the number of wavelengths to be digitally tuned is N, where $N=2^n$. The numbers of SOAs at the output side and the input are:

$$N_{output}=2^{n-1} \tag{10}$$

and,

$$N_{input}=2^{n-2} \tag{11}$$

respectively. The total number of SOAs is:

$$N_{total}=N_{input}+N_{output}=2^{n-2}+2^{n-1}=3 \cdot 2^{n-2} \tag{12}$$

In comparison with the structure reported in Ref(Glance,1996). and Ref(Zirngibl, 1994)., the proposed structure can save up 25% of SOAs for the same wavelength tuning range. The center wavelengths of the proposed DTOF are well in consistency with the ITU-T suggested

ones. Furthermore it does not have the thermal stability problem as the arrayed waveguide grating does (Hibino, 2002).

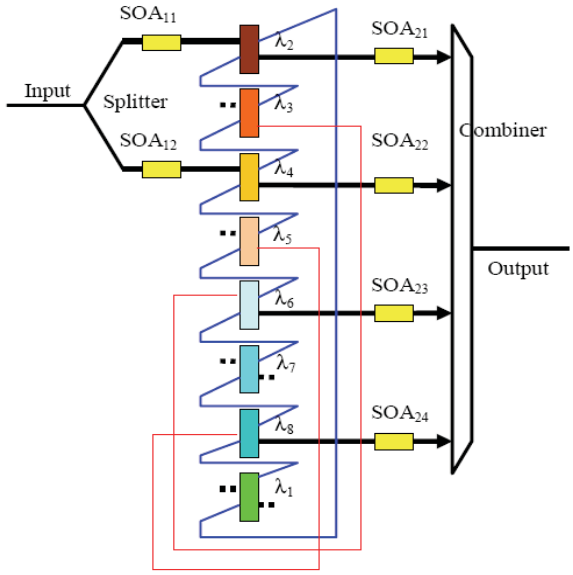

Fig. 13. The configuration of eight-channel digitally tunable optical filter

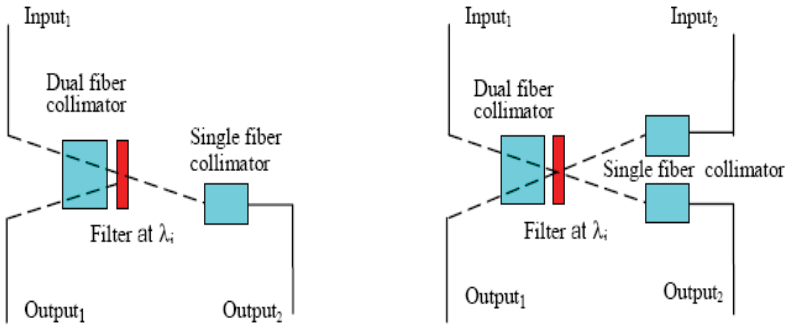

(a) 1×2 wavelength selection element (b) 2×2 wavelength selection element

Fig. 14. The structures of 1×2 and 2×2 wavelength selection elements

SOA_{11}	SOA_{12}	SOA_{21}	SOA_{22}	SOA_{23}	SOA_{24}	Selected wavelength at output
0	1	1	0	0	0	λ_1
1	0	1	0	0	0	λ_2
1	0	0	1	0	0	λ_3

0	1	0	1	0	0	λ_4
0	1	0	0	1	0	λ_5
1	0	0	0	1	0	λ_6
1	0	0	0	0	1	λ_7
0	1	0	0	0	1	λ_8

Table 3. The control table of the proposed DTOF (control states of SOAs:"1" stands for ON; "0" for OFF)

4.2 The performance of this digitally tunable filter

Fig. 15 is the transmission spectrum of the proposed DTOF. Its performance is list in Table 4 and 5. The eight wavelengths range from 1552.54nm to 1558.14nm. Table 4 lists the insertion loss for each wavelength channel. The maximum difference of the insertion loss among all eight wavelength channels is 3.76dB. The drive current of each SOA was set at 80mA for the "ON" state. The insertion loss difference can be compensated by optimizing the SOA drive current. In Table 5, the polarization dependent loss is less than 0.4dB and the isolation is better than 40 dB. The relatively large polarization dependent loss is partially induced by SOA. Another contribution may arise from the angled incidence on TTF (thin film filters) for its 1×2 and 2×2 application, which may decrease via careful design. The tuning speed was tested. It can be seen that the rise time and fall time of the optical response are 8.82 ns and 15.49 ns, respectively, and the delay time between the control signal and the optical response 31.07 ns. As is known, SOA has faster response than the measured results. This relatively larger rise/fall time and delay are mainly due to the poor response of the driving system which uses components at hand.

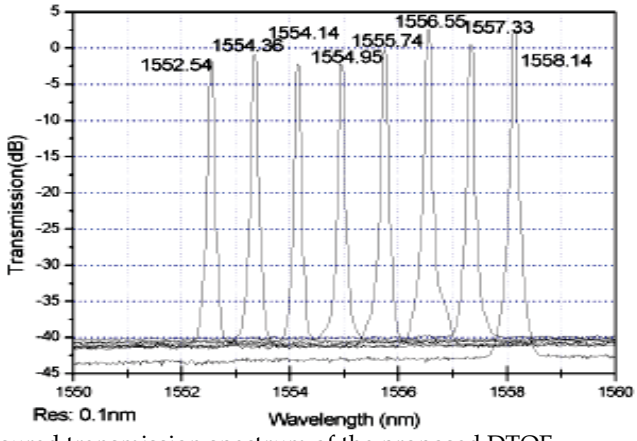

Fig. 15. The measured transmission spectrum of the proposed DTOF

Specification		Unit	Value	Notes
Polarization dependent loss		dB	< 0.4	Induced by SOA and the angled incidence on TTF
Isolation		dB	>40	
Tuning speed	Raise time	ns	<8.82	The poor response of driving system lead to this relatively larger
	Fall time	ns	<15.49	

				rise/fall time
Insertion loss		dB	In table 3	

Table 4. Specifications of the proposed DTOF

Wavelength (nm)	1552.54	1553.36	1554.14	1554.95
Insertion loss (dB)	5.94	5.56	6.67	6.9
Wavelength (nm)	1555.74	1556.55	1557.33	1558.14
Insertion loss (dB)	5.2	2.21	4.08	2.14

Table 5. The insertion loss for each wavelength channel

5. Digital wavelength selective optical switch

Digital wavelength selective optical switches (DWSS) have played an important role in wavelength-division-multiplexing (WDM) networking, and inspired widely research interest. Digital wavelength selective optical switch is a kind of optical switch which can make certain wavelengths from multiwavelength pass through or not according to the requirement of user(Li,2005). Several methods for optical switch have reported (Wang, 2006; Baxter, 2006; Goebuchi, 2006; Kishikawa, 2005). Optical switch based on those reported structure is polarization dependent, so strictly polarization control is necessary. In recently, we designed a new structure of wavelength selective optical switch based on Michelson interferometer, Faraday Rotation Mirror and Semiconductor Optical Amplifier.

5.1 The operating principle

Fig. 16 is the schematic for proposed digital wavelength selective optical switch. As shown in Fig. 16, it is divided into three sections: section I is a 1× N coupler; section II is constituted serials of fibre delay line, it's a key part, we can select the wavelengths we want by assembling different fibre delay line. In theory, C_N^2 wavelengths can be selected, if there are N fibre delay fibres; section III is the control part of this digital wavelength selective optical switch, according to the requirement two of the SOAs are turn on, then a set of wavelengths are selected and others turn off immediately.

Under normal operating state, only two SOAs would be turned on. So in fact, the proposed structure is a Michelson interferometer. And the transfer can be written as:

$$E_{out} = T_C \cdot T_D \cdot T_S \cdot T_{FM} \cdot T_S \cdot T_D \cdot T_C \cdot E_{in} \tag{13}$$

Where, E_{in} and E_{out} are the electric field complex amplitude of input and output light respectively; T_C, T_D, T_S and T_{FM} are the transfer matrixes of coupler, fibre delay lines, SOAs and Faraday rotation mirrors respectively. For simplifying the question, we assume the coupler is a 3dB direction coupler, and then those matrixes can be described as:

$$T_C = \begin{bmatrix} \sqrt{\alpha} & j\sqrt{1-\alpha^2} \\ j\sqrt{1-\alpha^2} & \sqrt{\alpha} \end{bmatrix} \tag{14}$$

Where, α is the splitting ratio of coupler.

$$T_D = \begin{bmatrix} \exp(-j\beta l_1) & 0 \\ 0 & \exp(-j\beta l_2) \end{bmatrix} \tag{15}$$

β is the propagation constant of light, l_1 and l_2 are the length of Michelson interference arms. Matrixes S and FM are identity matrixes.

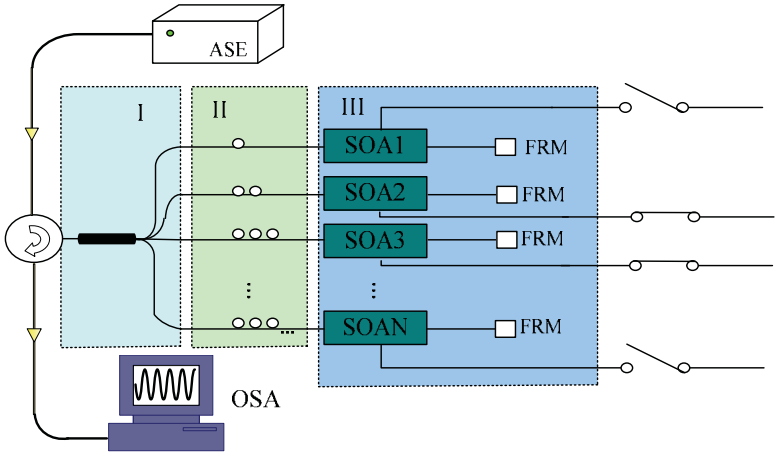

Fig. 16. Schematic of experimentally digitally wavelength selective optical switch.
SOA_N (N=1, 2, 3 …) is the Semiconductor Optical Amplifiers in the N^{th} interference arm; FRM is Faraday rotation mirror. ASE is a light source of Amplified Spontaneous Emission. OSA is an Optical spectrum analyzer.

It can be seen, from above expressions, the length difference between interference arms determine the selective wavelength. So the fibre delay lines play an important role in this device. Another important component of the device is Faraday rotation mirror, which consist of a 45° Faraday rotator and an ordinary mirror. It can automatically compensate for any polarization dependent effect. As a result, the wavelength selective optical switch is a polarization independent device.

5.2 Relation between the number of choice wavelength and insertion loss

With the increasing number of fibre delay line, as we know, the number of choice wavelength increase following the rule C_N^2. However, the insertion loss of this wavelength selective optical switch also increases.
According to the definition of insertion loss for optical switch, if the gain of SOAs is set at 0, the expression of insertion loss can be written theoretically as:

$$IL = -10\log_{10}\left(\frac{2}{N^2}\right) \text{ (dB)} \tag{16}$$

Where, IL is the insertion loss; N is the number of SOA.

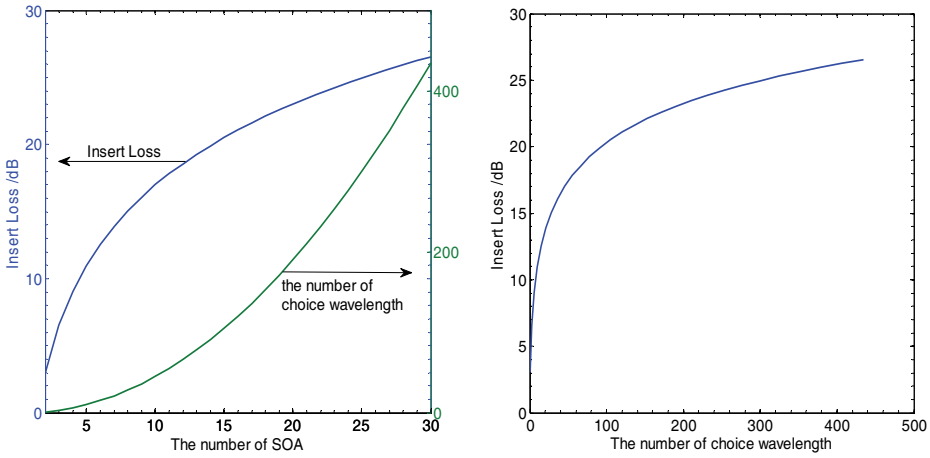

Fig. 17. Relation among N, number of choice wavelength and insertion loss

Fig. 17 shows the relation among N, number of choice wavelength and insertion loss. From it, we can see with the increase in the number of choice wavelength, the insertion loss also increase. So, the compromise between the number of choice wavelength and the insertion loss should be adapted in the design of this structure. Fig. 17 (left) shows the insertion loss is increasing with the number of SOA at exponential function and the number of choice wavelength at square function. Fig. 17 (right) shows the relationship between insertion loss and the number of choice wavelength, it indicates that the insertion loss began to increase rapidly, then slowly increased until stabilized with the number of choice wavelength. However in this structure, the insertion loss can be compensated by optimizing the SOA gain.

5.3 Performance measurement

Fig. 18 shows the transmission spectrum of our proposed digital wavelength selective optical switch. The operating wavelength is set at 1550.5 nm. While the difference between Michelson interferometer arms (ΔL) is 0.172 mm, the working state is "ON" as shown in Fig. 18 (a), otherwise the working state is "OFF" as shown in Fig. 18 (b).

Fig. 19 is the result of insertion loss for proposed DWSS (SOA1 and SOA2 gain> 0). As can be seen about four wavelengths are selective from the range of 1530 ~ 1560nm and the insertion loss of selective wavelengths are about -6 ~-2dBm.

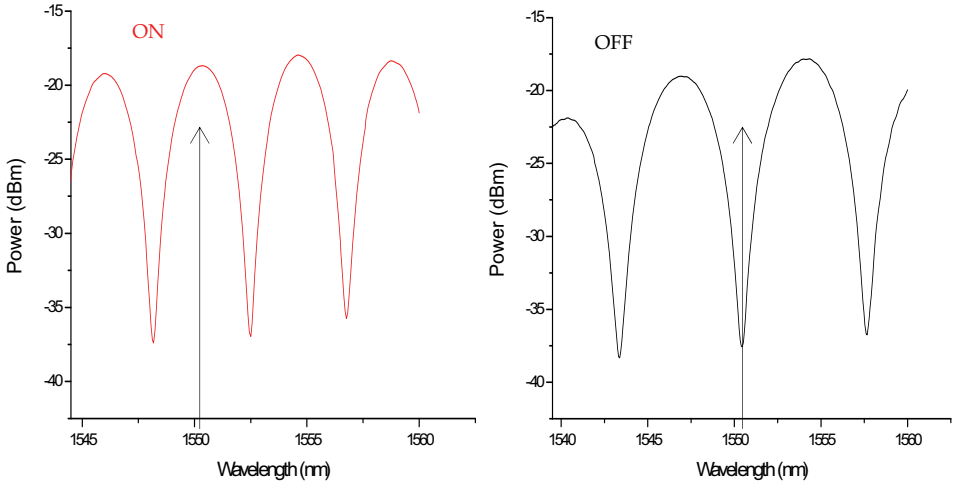

(a) ΔL=0.172 mm (b) ΔL =0.132 mm

Fig. 18. The transmission spectrum of proposed DWSS.
(ΔL: the difference between Michelson interferometer arms)

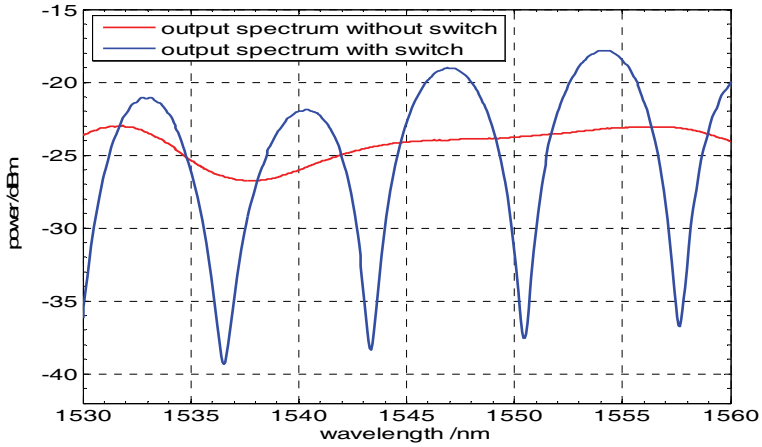

Fig. 19. Insertion loss of the proposed DWSS.
(The red line is output spectrum without switch and blue line with switch, the difference between two lines is the insertion loss of operating wavelength)

The response speed of proposed DWSS was test and the result is shown in Fig. 20. The red trace is control signal to drive SOAs, and the green trace is the response curve of the DWSS in time domain. It can be seen that rise time of the response curve is 65.05 ns. As is known, the response speed of SOA can achieve a few hundred picoseconds. So the relatively larger rise time is mainly owing to the poor response speed of the signal generator which generates the control signal in our measurement.

Fig. 20. Response speed of proposed DWSS

6. Micro/nano-photonic integration for VLSI photonics

The demand for higher communication speeds and greater capacity has grown exponentially. Especially, as the world entered the 21st century, it is experiencing an explosive increase which is driven by popular, bandwidth-hungry video applications (Nilsson, 2009).

Increase of communication capacity can be achieved by utilizing several resources including dense wavelength division multiplexing (DWDM), optical time division multiplexing (OTDM) and space division multiplexing techniques and so on. However, those techniques may encounter many technical bottlenecks, if the 40Gbit/s or 100Gbit/s transponders are launched largely. At present, it is a challenge for traditional discrete-component-based optical systems to drive down space and power per bit because the complex modulation techniques required for higher fibre capacity require a large number of optical and electronic components. To solve this question, micro & nano photonic integration was proposed recently due to photonic integration device have many crucial advantages comparing with discrete optical components(Nilsson, 2009), such as enabling rapid capacity addition in optical networks, reducing overall size and power consumption and improving reliability and so on.

Many progress of micro & nano photonic integration has been reported (Corzine, 2008; Ticknor, 2000; Park,2000). In March 23, 2009, Infinera has demonstrated photonic integrated circuits delivering 400 Gigabits/second (Gb/s) of optical capacity in a single pair of chips using complex modulation formats. It will enable Infinera's next generation optics to deliver up to 80% power savings over competitor 40 Gb/s wavelength optics based on conventional discrete optical components (Bob Blair, 2009).

On the other hand, photonic device based on micro/nano fibre has attracted widely attention owing to its characteristics of ultra-low-loss, compact structure and easily coupled with optic-fibre(Tong,2003; Brambilla, 2004; Yu, 2008). So the integrated photonics based on micro/nano fibre will provide a new way for very large-scale integration (VLSI) photonics. At present, our most efforts focus on the design and fabrication of photonics device based on micro/nano optic-fibre. Fig. 21 shows an architecture of the photonics integrated chip

based on micro/nano fibre(nf-PIC). In this chip most of function of an optical switching node can be realized. Next, we will simply introduce mainly micro/nano photonic device in this chip.

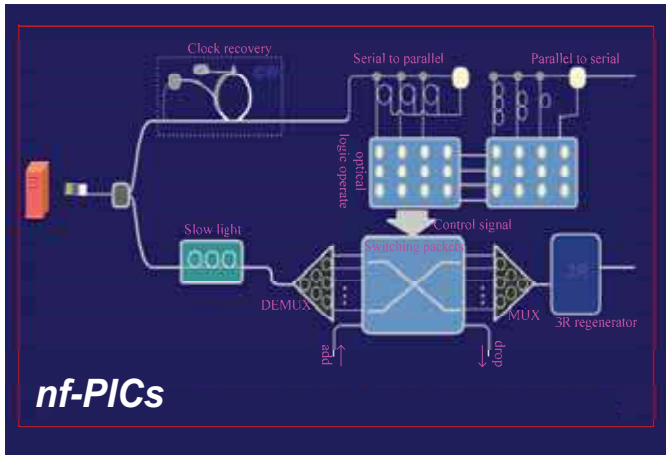

Fig. 21. Architecture of photonic integrated chip for optical switching node based on micro/nano fibre device (nf-PIC)

6.1 Micro/nano fibre taper

Fig. 21 doesn't show the details of each device, but it is play important role in photonic integrated chip. Optical signal transport in different devices maybe have different modes, so a mode adapter is necessary to convert one mode to another. Otherwise, the excess loss will be very large in high-density photonic integrated chip due to the mode mismatch. So, to min imize the excess loss in micro/nano photonic integrated chip, a kind of optimized low loss micro/nano fibre taper is an important device. This micro/nano fibre taper can meet the desire of low loss and compact structure in photonic integrated chip.

6.2 Clock recovery

Clock recovery is key element for communication system. In the proposed photonic integrated chip mode-locked lasers based on micro ring resonator will be adapted to achieve the function of clock recovery.

Fig. 22 shows the operation principle of clock recovery based on fibre microring resonator. While an optical pulse signal with cycle T pass through the nonlinear optical modulator, a period phased modulation is appeared in the laser due to cross-phase modulation effect, and output clock signal is synchronized with input signal.

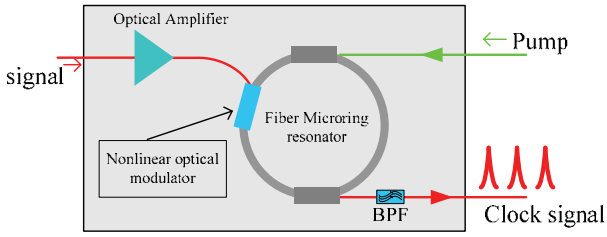

Fig. 22. Schematic of clock recovery. BPF: band-pass filter

6.3 Optical logic gate.

So far, almost the entire commercial logical device, its logic function is completed in electrical domain. As the development of higher speed and greater capacity communication, logic operation based on electronic component will don't encounter the demand owing to the bottleneck speed of electronic calculating. All-optical logic operation is one of choice to break the bottleneck speed of electronic component.

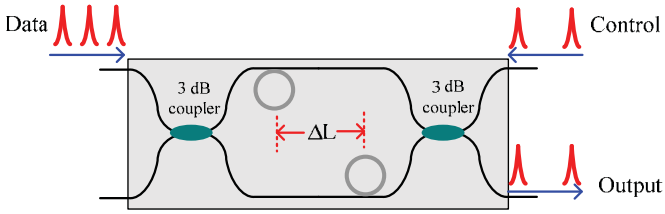

Fig. 23. AND logic gate based on microring and Mach-Zehnder interferometer

Fig. 23 addresses a kind of optical AND logic gate based on microring and Mach-Zehnder interferometer. On the one hand, if the control is "0" , the output will be "0" owing to the symmetrical arms of Mach-Zehnder interferometer; on the other hand, if the control and data are "1" simultaneously, the symmetrical structure will be break, then the output will be "1". Table 6 shows the truth table of this logic gate.

Control	Data	Output
0	0	0
0	1	0
1	0	0
1	1	1

Table 6. The truth table

6.4 Slow light

Slow light is a promising solution for memory, buffering and time domain processing of optical signal. There are many procedures to control velocity of light, one of is arrays of microrings resonator. Arrays of microring based on Micro/nano fibre have good prospects for generating slow light because they are compact, low loss and higher nonlinear effect, and can offer wide-bandwidth propagation.

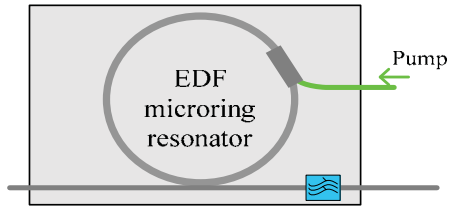

Fig. 24. Delay time tunable device for slow light

Accroding to Kramers-Kronig relationship, as long as there are Gain or transparency window, the slow light phenomenon will appear. So the resonator, such as microring , fibre grating and Fabry-perot, can generate slow light in its transparency window.
Microring shown in Fig. 24 can realize the function of delay time tunable because the ring was fabricated by Doped-Erbium Fibre, so the loss can be tunable of the ring, and the loss of microring resonator is one of a factor which can influence the delay time. As a result, we can tune the delay time by change the gain of EDF.

6.5 MUX/DEMUX

MUX/DEMUX is used frequently in optical communication system. Many techniques are adapted to fabricate MUX/DEMUX, such as optical lens, interferometric filter, holographic grating, fibre grating, waveguide grating, Mach-Zehnder interferometer and array waveguide grating and so on. But those structures are not easy to be integrated on chip. Arrays of fibre microrings due to the characteristic of high-Q, high finesse and compact structure and the convenience integrated on chip will be adapted on our proposed photonic integrated chip.
Fig. 25 shows a wavelength demultiplexer, it can also serve as wavelength multiplexer. The structure of microring resonator determines the wavelength which can set up resonance in microring, so multi-wavelength signal can be demultiplied by arrays of microring resonator.

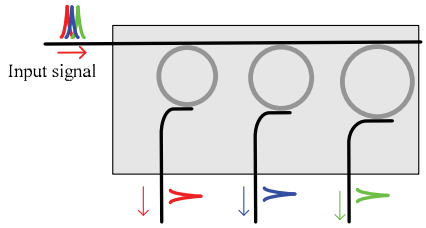

Fig. 25. Schematic of wavelength demultiplexer.(It also can be served as wavelength multiplexer.)

6.6 Optical switching

It is the core component in our proposed photonic integrated chip. The switching packets of this chip is achieved finally just by the optical switching. With the characteristics of microring, integrated arrays of fibre microring can also finish the optical switching with excellent performance.

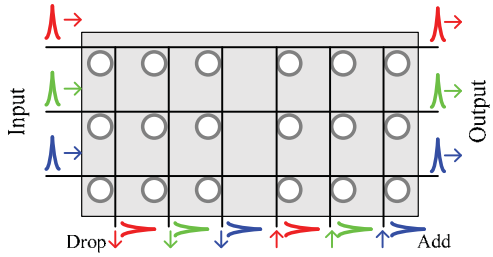

Fig. 26. Reconfigurable optical add-drop multiplexing

Fig. 26 shows a structure of reconfigurable optical add-drop multiplexing (ROADM) based on arrays of fibre microring resonator. Demultiplexed wavelength signals are input into ROADM, some of them pass through the ROADM, others dropped from drop port while the corresponding microrings are turned on by control signal. At the same principle, the wavelength can also be added in add port.

7. Conclusion

This chapter includes six sections. Except for the section of introduction, we will give brief conclusion the left five sections as follows:

In the second section, we introduced a new kind of 3^n feed-forward optical fibre delay lines. Theoretical analysis shows that it can provide large delays and is easy to be expanded. Experimental demonstration to implement such delay lines using SOAs and Farady rotation mirrors is presented. Delay step as small as 0.5 ps with precision of about 0.03 ps was realized. Measured results verify the feasibility of the proposed method. Its excellent expandability, low insertion loss, low polarization dependence loss and high tuning speed are suitable for application in phase array radar system and microwave signal processing.

Based on the structure above, we introduced a new kind of buffering structure by embedding 3^J feed-forward optical fibre delay lines into a re-circulating loop in the third section. Measurements have been carried out and the results have shown the fine property.

In the fourth section, a novel structure of eight-channel digitally tunable optical fibre based on thin film filters and semiconductor optical amplifiers has been demonstrated. The tuning speed is up to 8.82ns, the total insertion loss is between 2.14dB and 6.76dB. The isolation is over 40dB. The number of SOAs used in the proposed configuration is $3\times 2^{(\log_2 N)-2}$ where N is the number of tuned wavelengths. This means that the structure can save up 25% SOAs in comparison with the conventional digitally tunable optical filters. It can be expanded to large size with no additional insertion loss. Its wavelengths are well agreed with the defined ones by ITU-T and its temperature performance is stable. This kind of filter has potential application in wavelength selective switching based optical networks.

In the fifth section, a novel structure of digitally wavelength selective optical switch based on Michelson interferometer and semiconductor optical amplifiers has been demonstrated. The response speed is up to 65.05ns, the insertion loss is between -6 dB and -2 dB. In this structure, Faraday rotation mirrors are adapted, which can automatically compensate for any polarization dependent effect. As a result, the wavelength selective optical switch is a polarization independent device.

Many techniques for photonic integration have been reported. In the sixth section, we proposed another way based on micro/nano fibre device for VSLI photonics. Micro/nano-photonic integration is exhibiting its superiority in almost all of aspects of optical information process and communication technology. We hope the Micro/nano-photonic integration will achieve great success in 21st century like what the microelectronics had gain in 20th century.

8. Acknowledgement

This work was supported partially by National Science Foundation of China (NSFC) (ID60877012), 863 Project (ID2006AA01Z242 and 2007AA01Z275), Dawn Program for Excellent Scholars by the Shanghai Municipal Education Commission, the Key Disciplinary Development Program of Shanghai (T0102), HangTian Innovation Foundation and National Key Lab special Projects(GKZD030004). The authors are with the State Key Laboratory on Advanced Optical Communication Systems and Networks, Shanghai Jiao Tong University, Shanghai, China (e-mail: lixinwan@sjtu.edu.cn)

9. References

A. J. Seeds, K. J. Williams. (2006). Microwave photonics, *Journal of Lightwave Technology*, Vol 24, No.12,pp .4628–4641

J. Capmany, B. Ortega, D. Pastor, S. Sales, (2005). Discrete-time optical processing of microwave signals, *Journal of Lightwave Technology*, Vol. 23, No.2, pp .702-723

K. Wilner and A. P. Van Den Heuvel. (1976). Fibre-optic delay lines for microwave signal processing, *Proc.IEEE* ,Vol 64, No.5, pp.805–807

G. K. Chang, J. J Yu, Y. K. Yeo, A. Chowdhury, Z. S. Jia. (2006). Enabling technologies for next-generationoptical packet-switching networks, *Proceedings of the IEEE*, Vol 94, No.5, pp .892-910

A. J. Seeds. (2002). Microwave photonics, *IEEE Transactions on Microwave Theory and Techniques* . Vol 50, No.3, pp .877–887

E. J. Murphy, T. O. Murphy, A. F. Ambrose, R. W. Irvin, B. H. Lee, P. Peng, G. W. Richards, A.Yorinks. (1996). 16×16 strictly nonblocking guided-wave optical switching system, *Journal of Lightwave Technology* ,Vol 14, No.3, pp .352– 358

Y.K. Yeo, J. J. Yu, G. K. Chang. (2004). A dynamically reconfigurable folded-path time delay buffer for opticalpacket switching, *IEEE Photonics Technology Letters*, Vol 16, No.11, pp .2559 – 2561

B. Moslehi. (1992). Fibre-optic filters employing optical amplifiers to provide design flexibility, *Electronics Letters* , Vol. 28, No.3, pp .226–228

J. Capmany, B.Ortega, D. Pastor. (2006). A tutorial on microwave photonic filters, *Journal of Lightwave Technology* ,Vol 24, No.1,pp.201–229

A. Ho-Quoc, S. Tedjini, A. Hilt. (1996). Optical polarization effect in discrete time fiber-optic structures for microwave signal processing, *IEEE MTT-S International Microwave Symposium Digest*, Vol. 2, pp.907–910

D.J. Blumenthal, P. R. Prucnal, J. R .Sauer. (1994).Photonic packet switches: architectures and experimental implementations, *Proceedings of the IEEE* , Vol. 82, No.11, pp. 1650–1667

C.H. Shi, J.P. Chen, G.L. Wu, X.W.Li. (2006). Stable dynamic detection scheme for magnetostrictive fiber-optic interferometric sensors, *Optics. Express* .Vol.14, No.12. pp .5098-5102, http://www.opticsinfobase.org/abstract.cfm?URI=oe-14-12-5098

X.W. Li, L.M. Peng, S.B. Wang, Y.-C. Kim, J.P. Chen. (2007). A novel kind of programmable 3^n feed-forward optical fiber true delay line based on SOA,*Optics Express*, Vol.15, No.25, pp .16760-16766, http://www.opticsinfobase.org/oe/abstract.cfm?URI=oe-15-25-16760

Xinwan Li, Limei Peng, Jianping Chen, Songbo Wang, Guiling Wu, Jialin Lu, Young-Chon Kim. (2008) A novel fast programmable optical buffer with variable delays, *OFC/NFOEC* 2008,paper JThA41

Xinwan Li, Jianping Chen, Guiling Wu, Ailun Ye. (2005) , Digitally tunable optical filter based on DWDM thin film filters and semiconductor optical amplifiers, Optics. Express, Vol. 13, No. 4, *pp.* 1346-1350

D.Sadot. (1998). Tunable optical filters for dense WDM networks. *IEEE Commun. Magn*,Vol.**36**, No.12. pp .50–55

O.Ishida. (1997). Digitally tunable optical filters using arrayed-waveguide grating (AWG) multiplexers and optical switches. *Journal of Lightwave Technology,* Vol.**15**, No.2.pp. 321–327

B.Glance. (1996). Wavelength-tunable add/drop optical filter. *IEEE Photonics Technology Letters*, Vol.8, No.2.pp. 245–247

M.Zirngibl.(1994). Digitally tunable channel dropping filter/equalizer based on waveguide grating router and optical amplifier integration. *IEEE Photonics Technology Letters,* Vol.6, No.4, pp. 513–515.

B.Glance. (1994). Applications of the integrated waveguide grating router. *Journal of Lightwave Technol*ogy , Vol.12**,** No.6**,**pp. 957–962

Yoshinori Hibino. (2002). Recent advances in high-density and large-scale AWG Multi/demultiplexers with higher index-contrast silica-based PLCs. *IEEE J. Sel. Top. Quantum Electron,*Vol.8, No.6, pp. 1090-1101

Li X.W., Chen J. P., Wu G.L, Wang H., Ye A. L, (2005),An experimental study of an optical burst switching network based on wavelength-selective optical switches, *IEEE Communications Magazine*, Vol. 43, No.5, pp. S3-S10

Fan Wang, Jianyi Yang. & Limei Chen. (2006). Optical switch based on multimode interference coupler. *IEEE Photonics Technology Letters,* Vol. 18, No. 2, pp .421-423

Glenn Baxter, Steven Frisken. & Dmitri Abakoumov. (2006)**.** Highly programmable wavelength selective switch based on liquid crystal on silicon switching elements, *Proceedings of OFC/NFOEC 2006*, OTuF2, Anaheim, California, USA, 2006, California.

Yuta Goebuchi, Tomoyuki Kato. & Yasuo Kokubun. (2006). Fast and stable wavelength-selective switch using double-series coupled dielectric microring resonator. *IEEE Photonics Technology Letters*, Vol. 18, No. 3, pp . 538-540

Hiroki Kishikawa. & Nobuo Goto. (2005). Proposal of all-optical wavelength-selective switching using waveguide-type Raman amplifiers and 3-dB couplers. *Journal of Lightwave Technology,* Vol. 23, No. 4, pp .1631-1636

Alan C. Nilsson, Geoffrey S. Bennett. & David F. Welch. (2009). Advanced photonic integration and the revolution in optical networks, *Proc. of SPIE,* Vol. 7221, pp. 722102-1-722102-5

S. Corzine ; P. Evans. & M. Kato. (2008). Photonic integrated circuits for phase modulation formats, *Proceedings of IEEE Lasers and Electro-Optics Society. LEOS 2008. 21st Annual Meeting of the*, pp.334-335

Ticknor, A., Lipscomb, G.F. (2009). Passive PICs are key elements in 40- and 100-Gbps systems, *Lightwave* ,Vol.26, No.3, pp. 7-12

Park, S.-G. & Spiekman. (2000). Chirp consequences of all-optical RZ to NRZ conversion using cross-phase modulation in an active semiconductor photonic integrated circuit, *IEEE Photonics Technology Letters* ,Vol.12, No.3, pp. 233-235

Bob Blair, Jeff Ferry, (2009), Infinera's 400 Gb/s PIC sets new record for integration, release at website http://www.infinera.com/j7/servlet/NewsItem?newsItemID=150

Limin Tong, Rafael R. and Gattass. (2003). Subwavelength-diameter silica wires for low-loss optical wave guiding, *Nature* , Vol. 426 pp.816-819

Gilberto Brambilla,Vittoria Finazzi. & David J. Richardson. (2004). Ultra-low-loss optical fiber nanotapers, *Optics Express,* Vol.*12,* No.*10,* pp. *18-23*

Wu Yu, Zeng Xu. and Hou Changlun. (2008). A tunable all-fiber filter based on microfiber loop resonator, *Applied Physics Letters,* Vol.92, No.19, pp. 11-12.

Optical Fiber New Developments

Edited by Christophe Lethien

ISBN 978-953-7619-50-3
Hard cover, 586 pages
Publisher InTech
Published online 01, December, 2009
Published in print edition December, 2009

The optical fibre technology is one of the hop topics developed in the beginning of the 21th century and could substantially benefit applications dealing with lighting, sensing and communication systems. Many improvements have been made in the past years to reduce the fibre attenuation and to improve the fibre performance. Nowadays, new applications have been developed over the scientific community and this book fits this paradigm. It summarizes the current status of know-how in optical fibre applications and represents a further source of information dealing with two main topics: the development of fibre optics sensors, and the application of optical fibre for telecommunication systems.

How to reference

In order to correctly reference this scholarly work, feel free to copy and paste the following:

Xinwan Li, Zehua Hong, Shuguang Li and Jianping Chen (2009). Digitally Fast Programmable Optical Signal Processing Devices, Optical Fiber New Developments, Christophe Lethien (Ed.), ISBN: 978-953-7619-50-3, InTech, Available from: http://www.intechopen.com/books/optical-fiber-new-developments/digitally-fast-programmable-optical-signal-processing-devices

INTECH
open science | open minds

InTech Europe
University Campus STeP Ri
Slavka Krautzeka 83/A
51000 Rijeka, Croatia
Phone: +385 (51) 770 447
Fax: +385 (51) 686 166
www.intechopen.com

InTech China
Unit 405, Office Block, Hotel Equatorial Shanghai
No.65, Yan An Road (West), Shanghai, 200040, China
中国上海市延安西路65号上海国际贵都大饭店办公楼405单元
Phone: +86-21-62489820
Fax: +86-21-62489821